




## Numerical study of thermophysical characteristics of a cryogenic surface

M.S. Tazhenova<sup>1\*</sup> , R.R. Sultan<sup>1</sup>  and K.A. Katpayeva<sup>2</sup> 

<sup>1</sup>Al-Farabi Kazakh National University, Almaty, Kazakhstan

<sup>2</sup>Khoja Akhmet Yassawi International Kazakh-Turkish University, Turkestan, Kazakhstan

\*e-mail: marzhan.tazhen@gmail.com

(Received February 12, 2023; received in revised form March 20, 2023; accepted April 28, 2023)

This article is devoted to the development of a universal cryo surface for cooling and further work with active samples of various compositions in the surface temperature range of 80 K – 300K. To build a computer model of a universal cryo surface, the finite element method was used, which has a deep theoretical justification and is used to solve a wide range of problems. range of tasks. In the work, a computer model of a universal cryo surface with automatic maintenance of a given temperature in the range from 80 K to 300 K was created, which is intended for efficient production, taking into account all possible wishes of the system user and solving a wide range of problems. In the course of the study, working drawings of the cryo surface were obtained, a computer model of a universal cryo plate was developed, and thermophysical processes in it were studied. Based on the created mesh of the model and the results of the consumption of the working cryo-liquid, the optimal temperature values of the cryo surface were determined. With the help of this development, the problems of innovative materials processing technologies will be solved when creating a heat exchanger and substrate, creating an efficient pump for cryo-liquid, as well as creating a temperature maintenance system of various accuracy. The result will be a system with compactness, versatility, and autonomy.

**Key words:** cryo surface, nitrogen, finite element method, temperature, modeling.

**PACS numbers:** 64.60.-i; 78.20.Bh

### 1 Introduction

Cryogenic line refrigeration is the process of cooling a cryogenic liquid transfer line, typically from room temperature to cryogenic temperature, to ensure that the cryogenic liquids reach their destination in a liquid state. This process has attracted attention as cryogenic liquids play an increasingly important role in modern industries and academic fields [1-6]. During the cooling process of the line, a large amount of gas is inevitably generated, and this is often accompanied by a pressure surge phenomenon that can cause great damage to the system. Therefore, it becomes an integral part of cryogenic fluid management, which is a critical precondition for providing a stable and safe operating environment for a cryogenic system. The biggest challenge in cryogenic line cooling is to understand the heat transfer transient characteristics and predict the cooling process [7-9].

The heat transfer mode at each point in the transmission line changes over time as the flow pattern changes with wall temperature and fluid quality (Figure 1). However, imaging devices are difficult to implement at cryogenic temperatures. Changes in heat transfer patterns during the cooling process of a cryogenic line are often identified based on heat flow data obtained from measured wall temperature data.

Figure 2 shows a typical change in heat flow and heat transfer mode as the wall temperature changes. As we can see, while the wall is cooled by the cryogenic liquid flow, the heat transfer modes occur in the following order: single-phase gas convection, film boiling, transition boiling, nucleate boiling, and single-phase liquid convection. Parameters such as critical heat flux, temperature, and minimum heat flux, which are the boundary conditions for two boiling regimes, are commonly used to determine instantaneous boiling regimes [10-13].

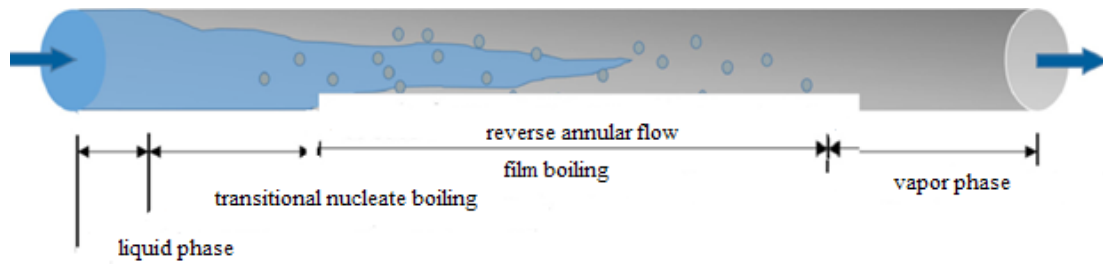


Figure 1 – Typical flow patterns and heat transfer modes during the cooling of a cryogenic line

However, some heat transfer modes may not be possible due to the condition of the pipeline and the properties of the fluid. For example, single phase gaseous convection occurs in a relatively long transmission line as the vaporized stream from the upstream, which is still colder than the pipe wall, slowly cools down the transmission line [14, 15].

On the contrary, film boiling is often considered as the beginning of the cooling process on a short transport line. Cooling of liquid hydrogen has been found starting from the transitional boiling regime under the condition of a very high Reynolds number, which is caused by its special properties [16-21].

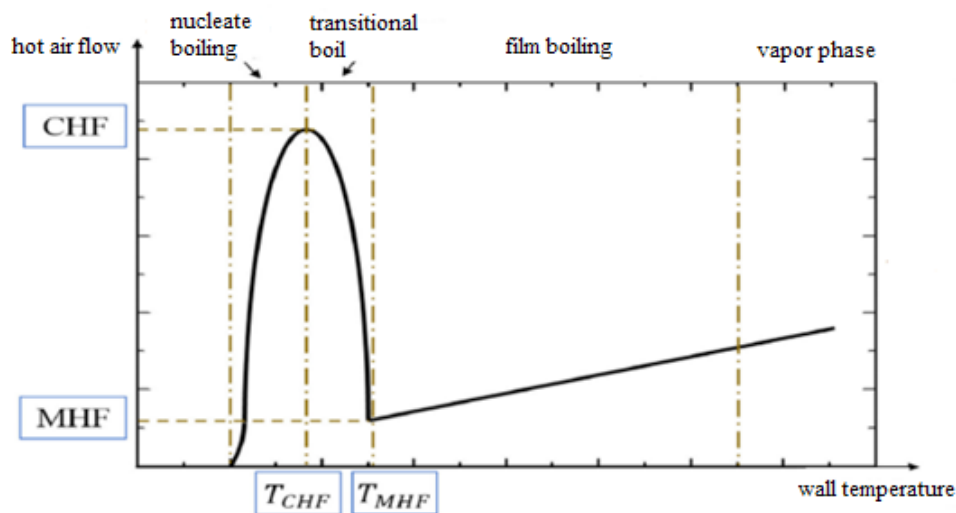


Figure 2 – Change in heat flux depending on the wall temperature

Advances in the cryogenic field allow for pumps based on this principle because of the promising means of achieving high vacuum levels. These pumps are usually called cryogenic vacuum pumps.

Particular attention in the design of cryopumps should also be paid to solving a number of cryotechnical issues, namely, ensuring a minimum thermal load on the cold elements of the pumps while ensuring the required pumping speed, since their efficiency largely depends on this. In cryogenic devices, it is very important to take into account thermal deformations and ensure the tightness of the

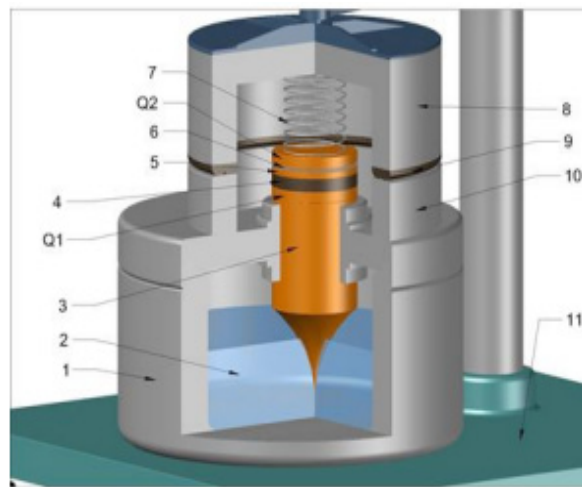
joints. It is also important to choose the method of cooling the cryo pump, which mainly determines the performance of the pump.

Important foreign developments in this area are the cryopanel for cryogenic vacuum pumps shown in Figure 3, but the tasks and applications of the cryopanel are completely different from the system of this project. Since the main task of the cryopanel is the creation of a vacuum. Whatever type of pump you use, the principle of creating a vacuum is the same. The vacuum is created by removing the gas molecule by molecule from the hermetically sealed working volume.

Cryogenic pipelines are used to transfer cryogenic liquid from the liquefier to the storage tank, as well as from the tank to the consumer. Cryogenic pipelines are supplied with high-quality vacuum thermal insulation, which reduces the volatility of the liquid. The required pressure is generated by the overpressure in the tank or pump. To cool special built-in cryopanel to 10K and 80K, on which gas molecules are actually deposited, the cryopump uses a closed cycle cooling system with helium as the working gas. Molecules of the pumped gas, moving randomly, come into contact

with the cryopanel and condense or are absorbed by them.

The outer row of gratings is cooled to 80K and used to condense water vapor, which is usually the main gas load. The inner row of condensation grates is cooled to a temperature of 15 K and is intended for the main part of the remaining gases. All condensable gases pass into a solid state at a vapor pressure of less than 10-12 Torr. Non-condensable gases such as helium, hydrogen and neon are simultaneously adsorbed by a layer of encapsulated activated carbon cooled to 15 K.



1 – Dewar vessel; 2 – liquid nitrogen; 3 – heat exchanger of the refrigerator; Q1 – lower cryostat; Q2 – upper cryostat; 4 – control sample; 5 – measuring plate; 6 – thermal conductivity standard; 7 – clamping spring; 8 – measuring cell cover; 9 – gasket; 10 – cell base; 11 – platform

**Figure 3** – Sketch of the measuring cell in the cut without using a cryopump

## 2 Mathematical model of the problem and methods

The finite element method (FEM) is the solution of problems by a numerical method, which can be either a minimization of a function or described by partial differential equations. Interest is presented as a set of finite elements. Finite elements have the same properties that define and reduce the number of unknowns. Approximation functions in finite elements are defined in terms of the key value of the specified physical field. The continuous physics problem is transformed into a discretized finite element problem with unknown key values. For linear algebraic equations, the problem must

be solved linearly. With the use of key values, the values within the finite elements can be retrieved [22-25].

Elements consisting of edges and nodes, which are interception points and links between elements, are the result of a split. The solution of differential equations with respect to a physical problem can be solved by approximate functions that satisfy the conditions described by integral equations in the problem domain. Such approximate functions are polynomial functions.

The features of this method include:

- When using simple approximating elements, we can achieve any accuracy of piecewise approximation of physical fields on finite elements;

- The locality of the approximation leads to systems of sparse equations for the discretized problem. It helps to solve problems with very large number of nodal unknowns.

Due to its advantages, piecewise approximation of physical fields is the most used form of solving the problem when solving complex geometry.

The removal of heat from the surface of an object of a universal cryogenic surface (UCS) is provided by the convection of the movement of the gaseous coolant flow and is described by the Navier-Stokes equations [26-28]:

$$\frac{\rho}{dt} + \nabla \cdot (\rho \mathbf{u}) = 0, \quad (1)$$

$$\rho \frac{d\mathbf{u}}{dt} + \rho(\mathbf{u} \cdot \nabla)\mathbf{u} = \nabla \cdot [-\rho\mathbf{I} + \boldsymbol{\tau}] + \mathbf{F}, \quad (2)$$

$$\begin{aligned} \rho C_p \left( \frac{dT}{dt} + (\mathbf{u} \cdot \nabla)T \right) = \\ = -(\nabla \cdot \mathbf{q}) + \boldsymbol{\tau} : \mathbf{S} - \\ - \frac{T}{\rho} \frac{d\rho}{dT} \left( \frac{d\rho}{dt} + (\mathbf{u} \cdot \nabla)\rho \right) + Q, \end{aligned} \quad (3)$$

where  $\rho$  is density,  $\mathbf{u}$  is velocity vector,  $p$  is pressure,  $\boldsymbol{\tau}$  is viscous stress tensor,  $\mathbf{F}$  is body force vector,  $C_p$  is specific heat capacity,  $T$  is absolute temperature,  $\mathbf{q}$  is heat flow vector,  $Q$  contains heat sources,  $\mathbf{S}$  is tensor strain rate.

Equation (1) is called the equation of continuity or continuity of the flow, it is an algebraic representation

similar to the conservation of mass. Equation (2) is a vector equation which represents the conservation of momentum. Equation (3) describes the conservation of energy, formulated in terms of temperature.

### 3 Results

In this work, a numerical model of the universal cryo surface was created. The number of elements varied depending on the geometry of the model, but on average it was about 30,500 finite elements, where the number of vertex elements was 20,000, the number of boundary elements was about 10,000, and the minimum element size into which the zone of the universal cryo surface is divided was 0.012 mm. The mesh was generated automatically thanks to the physics-controlled mesh customization. For a more complex configuration, custom grid settings can be used.

All material properties were taken as isotropic in the calculations of this model. The data on thermal conductivity and heat capacity used in the model are presented as a function of temperature. The materials used were steel, nitrogen and air.

The following figures show the results of modeling the universal cryo surface. Figures 4-8 show the temperature distributions in the 3D model of the universal cryo surface.

In Figure 4, we can observe the intensive cooling of the cryo surface over time. At the time of 30 seconds, we see that 90% of the surface of the universal cryo surface model is approaching 100 K.

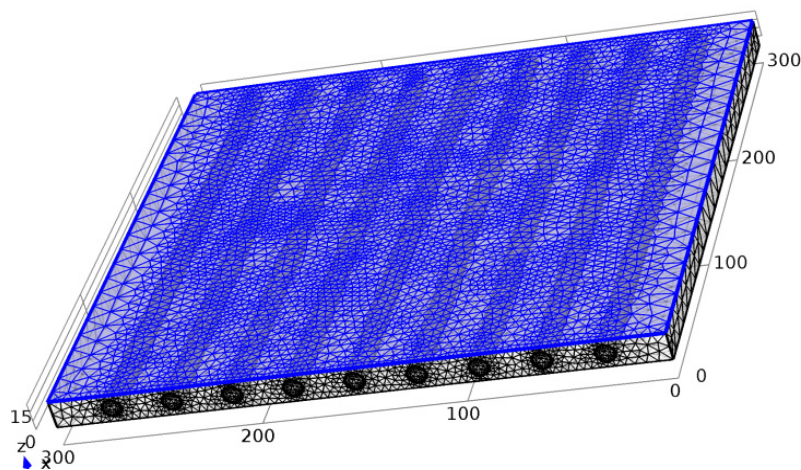


Figure 4 – General view of the model grid

The computer model of thermophysical processes in the model of a universal plate was implemented using the finite element method. The schematic model is shown in Figure 5.

The geometrical dimensions of the computer model of the CSM were equal to 300x300x15 mm.

Where holes with a diameter of 3/5/7 mm were made with a step of 30 mm from the centers of the holes.

The following figures 6-8 show the temperature distributions along the cryo surface at different times.

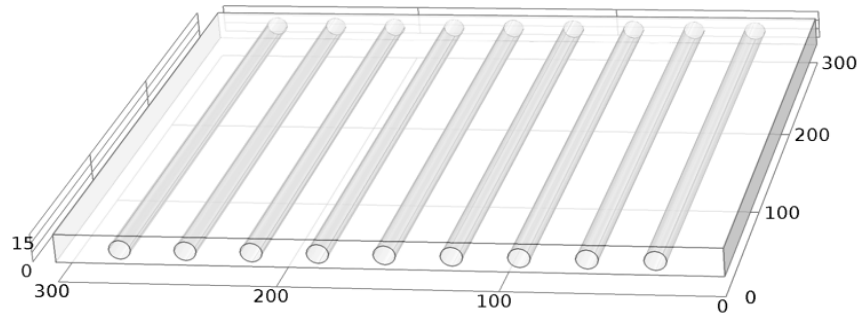


**Figure 5** – General view of the universal cryo surface model

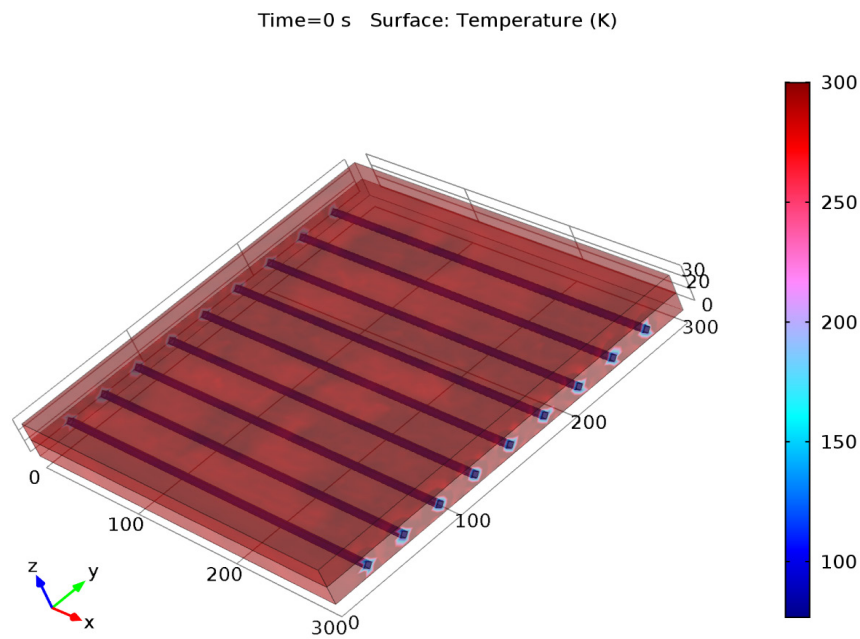


**Figure 6** – Temperature distribution along the cryo surface at the initial time t=0 s



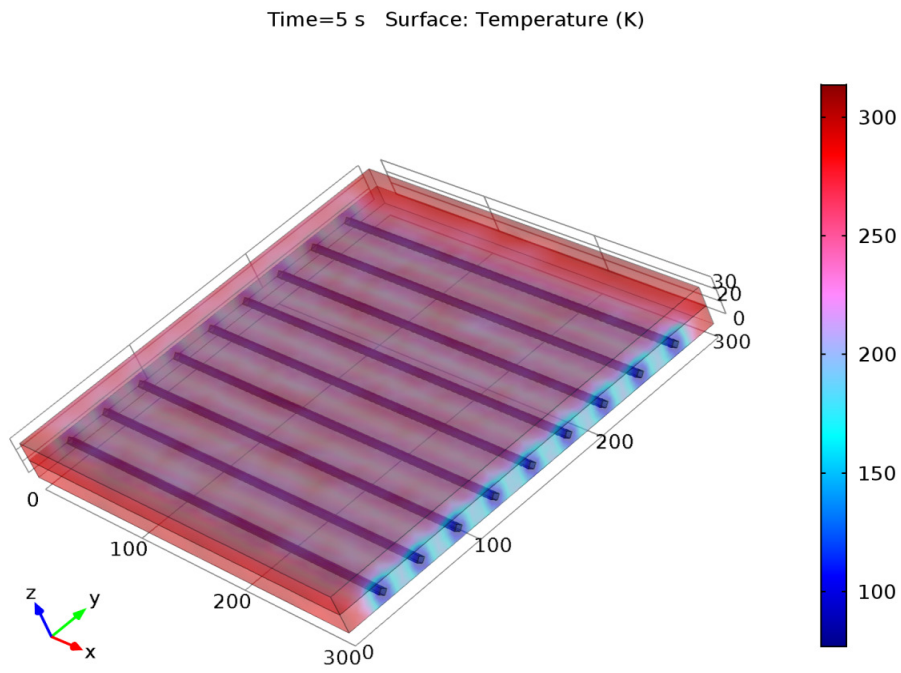


Figure 7 – Temperature distribution along the cryo surface at time  $t=5$  s

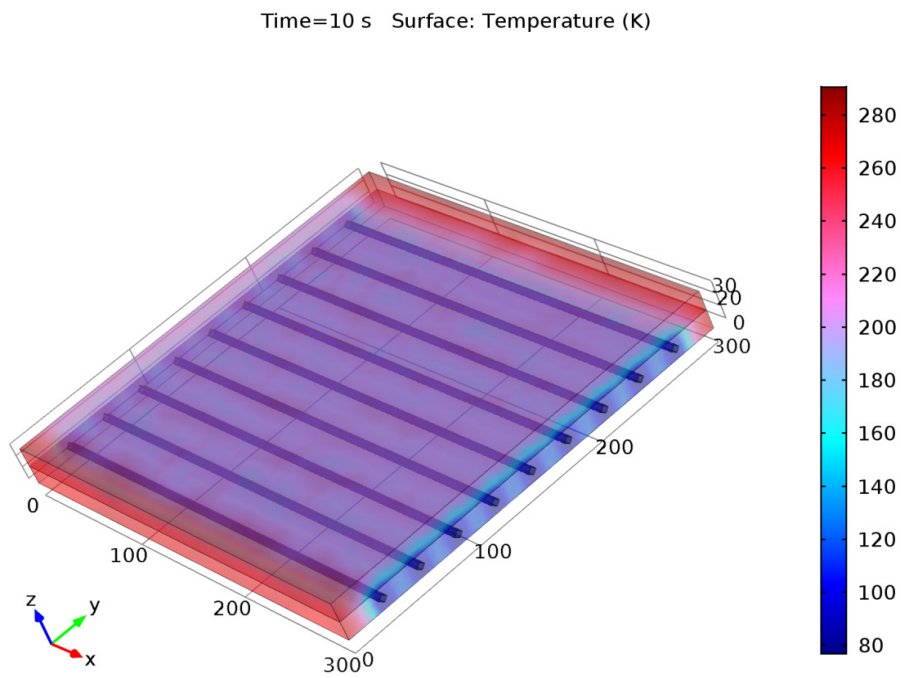
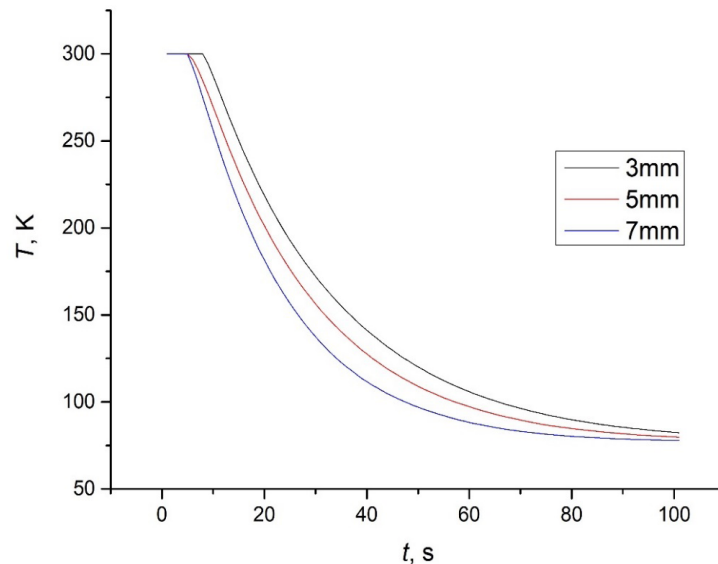


Figure 8 – Temperature distribution along the cryo surface at time  $t=10$  s

Figure 9 shows a graph of the distribution of the maximum temperature over the entire surface area of the model of the universal cryosurface. We can notice that when considering the maximum temperature

over the entire surface area, there is a clear effect of the diameter size of the heat exchange tube. More intensive cooling of the surface area of the cryo surface is observed at a heat exchange tube diameter of 7 mm.



**Figure 9** – Distribution of the maximum temperature over the cryo surface area over time

#### 4 Conclusions

In this work, in the course of numerical simulation, a model of a universal cryo surface was created. By means of the finite element method, geometric and physical models of the universal cryo surface were constructed. The temperature characteristics of a steel plate at various points in time were investigated.

According to the obtained results of computer simulation, it can be concluded that the computer model of the cryosurface obtained by us is adequate and retains the advantageous properties of the real cryo surface.

Based on the obtained results, we can draw the following conclusions:

- universal cryogenic surface reaches temperature equilibrium in 70 seconds in the case of a 7 mm hole diameter;

- in the case of 5 mm and 3 mm tube hole diameter, an increase in cooling time to 90 and 100 seconds, respectively, is observed;

- temperature distributions over the surface of a universal cryo plate are shown in the form of a 3D temperature model;

- the results of this study may contribute to the further development of cryogenic technologies in low temperature physics

The results obtained in the work are not only scientific, but also applied in nature and will be used in developments in various fields of science: when measuring thermal conductivity by the relative method, determining the viscosity of petroleum products, space research and low-temperature measurements; in medicine in the manufacture of drugs, the study of biological samples and the crystallization of protein compounds; in industry and for display repairs. This is necessary for the preferences of demand and the selection of the configuration of the invention without changing the overall design, and significant cost savings for the consumer.

## References

1. Baek S. et al. Novel design of LNG (liquefied natural gas) reliquefaction process // *Energy Conversion and Management*. – 2011. – Vol. 52, No. 8–9. – P. 2807–2814. <https://doi.org/10.1016/j.enconman.2011.02.015>
2. Joseph J. et al. Fluid-hammer induced pressure oscillations in a cryogenic feed line // *IOP Conference Series: Materials Science and Engineering*. – 2017. – Vol. 171. <http://dx.doi.org/10.1088/1757-899X/171/1/012049>
3. Hu H., Chung J.N., Amber S.H. An experimental study on flow patterns and heat transfer characteristics during cryogenic chilldown in a vertical pipe // *Cryogenics*. – 2012. – Vol. 52, No. 4–6. – P. 268–277. [https://ui.adsabs.harvard.edu/link\\_gateway/2012Cryo...52..268H/doi:10.1016/j.cryogenics.2012.01.033](https://ui.adsabs.harvard.edu/link_gateway/2012Cryo...52..268H/doi:10.1016/j.cryogenics.2012.01.033)
4. Johnson J., Shine S.R. Transient cryogenic chill down process in horizontal and inclined pipes // *Cryogenics*. – 2015. – Vol. 71. – P. 7–17. <https://doi.org/10.1016/j.cryogenics.2015.05.003>
5. Darr S.R. et al. An experimental study on terrestrial cryogenic tube chilldown II. Effect of flow direction with respect to gravity and new correlation set // *International Journal of Heat and Mass Transfer*. – 2016. – Vol. 103. – P. 1243–1260. <https://doi.org/10.1016/j.ijheatmasstransfer.2016.08.044>
6. Darr S.R. et al. An experimental study on terrestrial cryogenic transfer line chilldown I. Effect of mass flux, equilibrium quality, and inlet subcooling // *International Journal of Heat and Mass Transfer*. – 2016. – Vol. 103. – P. 1225–1242. <https://doi.org/10.1016/j.ijheatmasstransfer.2016.05.019>
7. Jin L., Cho H., Jeong S. Experimental investigation on line chill-down process by liquid argon // *Cryogenics*. – 2019. – Vol. 97. – P. 31–39. <https://doi.org/10.1016/j.cryogenics.2018.11.003>
8. Hartwig J. et al. Comparison of cryogenic flow boiling in liquid nitrogen and liquid hydrogen chilldown experiments // *International Journal of Heat and Mass Transfer*. – 2015. – Vol. 88. – P. 662–673. <https://doi.org/10.1016/j.ijheatmasstransfer.2015.04.102>
9. Hartwig J., Darr S., Asencio A. Assessment of existing two phase heat transfer coefficient and critical heat flux correlations for cryogenic flow boiling in pipe quenching experiments // *International Journal of Heat and Mass Transfer*. – 2016. – Vol. 93. – P. 441–463. <https://doi.org/10.1016/j.ijheatmasstransfer.2015.09.028>
10. Ganesan V. et al. Universal Critical Heat Flux (CHF) Correlations for Cryogenic Flow Boiling in Uniformly Heated Tubes // *International Journal of Heat and Mass Transfer*. – 2021. – Vol. 166. – No. 120678. <https://doi.org/10.1016/j.ijheatmasstransfer.2020.120678>
11. Muttakin M. et al. Study on optimized adsorption chiller employing various heat and mass recovery schemes // *International Journal of Refrigeration*. – 2021. – Vol. 126. – P. 222–237. <https://doi.org/10.1016/j.ijrefrig.2020.12.032>
12. Sheng B. et al. A corresponding state equation for compressed liquid isochoric heat capacity of pure and mixture refrigerants // *International Journal of Refrigeration*. – 2021. – Vol. 124. – P. 20–29. <https://doi.org/10.1016/j.ijrefrig.2020.12.016>
13. Liang G., Mudawar I. Review of pool boiling enhancement by surface modification // *International Journal of Heat and Mass Transfer*. – 2019. – Vol. 128. – P. 892–933. <https://doi.org/10.1016/j.ijheatmasstransfer.2018.09.026>
14. Mercado M., Wong N., Hartwig J. Assessment of two-phase heat transfer coefficient and critical heat flux correlations for cryogenic flow boiling in pipe heating experiments // *International Journal of Heat and Mass Transfer*. – 2019. – Vol. 133. – P. 295–315. <https://doi.org/10.1016/j.ijheatmasstransfer.2018.12.108>
15. Panão M.R.O., Moreira A.L.N., Durão D.F.G. Thermal-fluid assessment of multijet atomization for spray cooling applications // *Energy*. – 2011. – Vol. 36, No. 4. – P. 2302–2311. <https://doi.org/10.1016/j.energy.2010.05.042>
16. Wang F. et al. Diffusion thermodynamic behavior of milling Ti-6Al-4V alloy in liquid nitrogen cryogenic cooling // *The International Journal of Advanced Manufacturing Technology*. – 2018. – Vol. 95, No. 5–8. – P. 2783–2793. <https://doi.org/10.1007/s00170-017-1427-2>
17. Xue R. et al. Experimental study of liquid nitrogen spray characteristics in atmospheric environment // *Applied Thermal Engineering*. – 2018. – Vol. 142. – P. 717–722. <https://doi.org/10.1016/j.applthermaleng.2018.07.056>
18. Zhang R. et al. Investigation on the critical heat flux in typical 5 by 5 rod bundle at conditions prototypical of PWR based on CFD methodology // *Applied Thermal Engineering*. – 2020. – Vol. 179. – No. 115582. <https://doi.org/10.1016/j.applthermaleng.2020.115582>
19. Bruder M., Bloch G., Sattelmayer T. Critical Heat Flux in Flow Boiling—Review of the Current Understanding and Experimental Approaches // *Heat Transfer Engineering*. – 2017. – Vol. 38, No. 3. – P. 347–360. <https://doi.org/10.1080/01457632.2016.1189274>
20. Liang G., Mudawar I. Pool boiling critical heat flux (CHF) – Part 2: Assessment of models and correlations // *International Journal of Heat and Mass Transfer*. – 2018. – Vol. 117. – P. 1368–1383. <https://doi.org/10.1016/j.ijheatmasstransfer.2017.09.073>



21. Lee J., O'Neill L.E., Mudawar I. Computational prediction of key heat transfer mechanisms and hydrodynamic characteristics of critical heat flux (CHF) in subcooled vertical upflow boiling // *International Journal of Heat and Mass Transfer*. – 2020. – Vol. 161. – No. 120262. <https://doi.org/10.1016/j.ijheatmasstransfer.2020.120262>
22. Lee J., O'Neill L.E., Mudawar I. 3-D computational investigation and experimental validation of effect of shear-lift on two-phase flow and heat transfer characteristics of highly subcooled flow boiling in vertical upflow // *International Journal of Heat and Mass Transfer*. – 2020. – Vol. 150. – No. 119291. <https://doi.org/10.1016/j.ijheatmasstransfer.2019.119291>
23. Lee H. et al. Experimental and computational investigation of vertical downflow condensation // *International Journal of Heat and Mass Transfer*. – 2015. – Vol. 85. – P. 865–879. <https://doi.org/10.1016/j.ijheatmasstransfer.2015.02.037>
24. Kim Y.J. et al. Flow boiling CHF experiment with sudden expansion tubes // *International Communications in Heat and Mass Transfer*. – 2020. – Vol. 114. – No. 104557. <https://doi.org/10.1016/j.icheatmasstransfer.2020.104557>
25. O'Neill L.E., Mudawar I. Review of two-phase flow instabilities in macro- and micro-channel systems // *International Journal of Heat and Mass Transfer*. – 2020. – Vol. 157. – No. 119738. <https://doi.org/10.1016/j.ijheatmasstransfer.2020.119738>
26. Ferreira J., Kaviany M. Geometric-confinement suppression of flow-boiling instability using perforated wick: Part I CHF and conductance enhancement // *International Journal of Heat and Mass Transfer*. – 2020. – Vol. 159. – No. 120080. <https://doi.org/10.1016/j.ijheatmasstransfer.2020.120080>
27. Devahdhanush V.S. et al. Assessing advantages and disadvantages of macro- and micro-channel flow boiling for high-heat-flux thermal management using computational and theoretical/empirical methods // *International Journal of Heat and Mass Transfer*. – 2021. – Vol. 169. – No. 120787. <https://doi.org/10.1016/j.ijheatmasstransfer.2020.120787>
28. Cai C. et al. Assessment of void fraction models and correlations for subcooled boiling in vertical upflow in a circular tube // *International Journal of Heat and Mass Transfer*. – 2021. – Vol. 171. – No. 121060. <https://doi.org/10.1016/j.ijheatmasstransfer.2021.121060>